Biochimica et Biophysica Acta 1852 (2015) 2423–2431

Contents lists available at ScienceDirect

Biochimica et Biophysica Acta

journal homepage: www.elsevier.com/locate/bbadis

Brain targeted PLGA nanocarriers alleviating amyloid-B expression and preserving basal survivin in degenerating mice model

Bhasker Sriramoju [a], Prasad Neerati [b], Rupinder K. Kanwar [a], Jagat R. Kanwar [a,*]

[a] Nanomedicine Laboratory of Immunology and Molecular Biomedical Research (NLIMBR), School of Medicine, Faculty of Health, Deakin University, Waurn Ponds, Geelong, VIC 3216, Australia
[b] Department of Pharmacology, University College of Pharmaceutical Sciences, Kakatiya University, Andhra Pradesh, Warangal 506002, India

ARTICLE INFO

Article history:
Received 15 April 2015
Received in revised form 24 July 2015
Accepted 19 August 2015
Available online 21 August 2015

Keywords:
Alzheimer's disease
Advanced glycation end products
D-Galactose
Anti-transferrin receptor antibody
SurR9-C84A

ABSTRACT

The chronic systemic administration of D-Galactose in C57BL/6J mice showed a relatively high oxidative stress, amyloid-β expression and neuronal cell death. Enhanced expression of pyknotic nuclei, caspase-3 and reduced expression of neuronal integrity markers further confirmed the aforesaid insults. However, concomitant treatment with the recombinant protein (SurR9-C84A) and the anti-transferrin receptor antibody conjugated SurR9-C84A (SurR9 + TFN) nanocarriers showed a significant improvement in the disease status and neuronal health. The beauty of this study is that the biodegradable Food and Drug Administration (FDA) approved poly(lactic-co-glycolic acid) (PLGA) nanocarriers enhanced the biological half-life and the efficacy of the treatments. The nanocarriers were effective in lowering the amyloid-β expression, enhancing the neuronal integrity markers and maintaining the basal levels of endogenous survivin that is essential for evading the caspase activation and apoptosis. The current study herein reports for the first time that the brain targeted SurR9-C84A nanocarriers alleviated the D-Galactose induced neuronal insults and has potential for future brain targeted nanomedicine application.

1. Introduction

A chronic systemic administration of D-Galactose (D-Gal) induces the natural ageing process in animals characterized by the features of reduced lifespan [1,2], cognitive impairment [3,4], oxidative stress [5], compromised immunity [6], formation of advanced glycation end products (AGEs) [7,8] and neurodegeneration [9]. Added to this, aged individuals are reported to be much more susceptible to many of the chronic diseases such as the neurodegenerative type and the mitochondrial free radical toxicity [10]. A theory is also in existence which states that ageing and its associated disorders are a result of the free radical induced damage to the cellular components and that there exists no defence machinery with them to counteract this stress [11]. Eventually, the damaged mitochondria losses its integrity and becomes inefficient progressively, secreting more of the free radicals. Ageing is a substantial risk factor for the development of Alzheimer's disease (AD) which typically falls under the category of neurodegeneration. A probable clarification for this is that ageing positively influences the neuronal degeneration by enhancing the oxidative stress, protein accumulation, reducing their enzymatic clearance, and interrupting the calcium homeostasis affecting the mitochondrial functioning [12]. AGEs are a cluster of diverse compounds formed from the non-enzymatic catalysis of the reducing sugars (glucose, fructose *etc.*) with the amino acids present in proteins, DNA or lipids [13]. These AGEs were found to accumulate as the ageing progresses and are associated with a number of age related diseases such as neurodegeneration [14,15]. D-Galactose is one such compound obtained as a nutrient (*e.g.* lactose in milk) and synthesised in the body where it forms glycolipids and glycoproteins.

In general, it is metabolised by D-galactokinase and galactose-1-phosphate uridyltransferase to non-toxic compounds [5]. But, at levels above the normal range, it is metabolised to galactitol by aldose reductase that reacts abnormally with the amino acids forming AGEs [16]. Chronic D-Gal administration also activates the acetyl cholinesterase (AChE) activity which rapidly degrades the acetylcholine in the synaptic cleft. Subsequently, there is a decrease in the cholinergic stimulation that leads to an enhanced inflammatory response, tissue damage and cognitive impairment [17,18]. These symptoms characterise the AD generation with the hallmark representation of amyloid beta (Aβ) peptide extracellular deposition and intracellular neurofibrillary tangles [19]. Since, the chronic D-Gal administration induced senescence is associated with neurodegeneration it would, therefore, be an appropriate

Abbreviations: Aβ, amyloid beta; AchE, acetyl cholinesterase; AD, Alzheimer's disease; AGEs, advanced glycation end products; APP, amyloid precursor protein; BBB, blood brain barrier; D-Gal, D-Galactose; EAAT2, excitatory amino acid transporter 2; EDC, 1-ethyl-3-[3-dimethylaminopropyl]carbodiimide hydrochloride; GFAP, glial fibrillary acidic protein; GSK, glycogen synthase kinase; IAPs, inhibitor of apoptotic proteins; NF, neurofilament; NHS, N-hydroxysulfosuccinimide; PVA, poly vinyl alcohol; SurR9 + TFN, SurR9-C84A nanoparticles conjugated to anti-transferrin receptor antibody.

* Corresponding author at: Nanomedicine-Laboratory of Immunology and Molecular Biomedical Research (NLIMBR), School of Medicine (SoM), Centre for Molecular and Medical Research (C-MMR), Faculty of Health, Deakin University, Geelong Technology Precinct (GTP), Pigdons Road, Waurn Ponds, Geelong, Victoria 3216. Australia.
E-mail address: jagat.kanwar@deakin.edu.au (J.R. Kanwar).

http://dx.doi.org/10.1016/j.bbadis.2015.08.015
0925-4439/

model for understanding the molecular mechanisms of ageing associated AD. On the other hand, delivery of therapeutic compounds to the brain is always challenging due to the presence of the blood brain barrier (BBB). Only the compounds possessing small molecular mass below the 400 Da size and high lipophilicity can cross it and satisfying these requirements for a conventional therapeutic is quiet difficult. Hence, the ideal way to deliver the drugs is to encapsulate them inside the nanoparticles and customise them with the brain specific markers. This would eventually enhance the bioavailability and protect them from enzymatic degradation, enabling the delivery of maximum pay load [20,21]. The poly (lactic-co-glycolic acid) (PLGA) polymer has been used for the preparation of nanoparticles on account of its bio-compatibility and feasibility for surface functionalization. The PLGA nanoparticles have gained enormous reputation for the formulation of several drugs and also were approved by the US Food and Drug Administration (FDA) for clinical application [22–25].

In the present study, D-Gal (120 mg/kg) was administered to the animals to induce neuronal injury mimicking the ageing associated AD. The activities of the mutant protein SurR9-C84A and its targeted formulation have not been tested before in the D-Gal induced AD model. The mutant SurR9-C84A is a recombinant protein that belongs to the family of inhibitor of apoptosis proteins (IAPs) family and shows bi-functional activity (apoptotic or mitotic) depending on the basal levels of wild type survivin [24]. In summary, the current study aimed to investigate the neuroprotector activity of SurR9-C84A protein and compared them against the positive control melatonin. Melatonin (N-acetyl-5-methoxytryptamine) is a hormone secreted from the pineal gland and it acts against ageing because of its ability to mitigate mitochondrial malfunction and oxidative stress [26].

2. Materials and methods (see supplementary Section 1)

2.1. Nanoparticle preparation and characterization

The SurR9-C84A loaded PLGA nanoparticles (NPs) were prepared and characterized as described earlier [27]. In brief, a 1% w/v of PLGA polymer in ethyl acetate was prepared and added to the 1% polyvinyl alcohol (PVA) containing 10 mg/ml of protein to give the initial W/O emulsion. Then, the final volume of 15 ml of PVA was added to yield the W/O/W emulsion which was stirred at 800 RPM overnight at 4 °C to yield the NPs. Later, they are centrifuged, collected, freeze dried and stored for future use. The void NPs used for the *in vivo* study were prepared using the same procedure except that they were devoid of the proteins used. The transferrin receptor antibody conjugated SurR9-C84A loaded targeted NPs were prepared using the carbodiimide chemistry. In this technique, the free carboxyl groups of the PLGA NPs were incubated with the 0.1 M 1-ethyl-3-[3-dimethylaminopropyl] carbodiimide hydrochloride (EDC) and 0.7 M N-hydroxysulfosuccinimide (NHS) mix for 4 h at RT. Following this, the surface activated NPs were incubated with mouse monoclonal transferrin receptor antibody (OX26, Santa Cruz) overnight at 4 °C. The next day, nanoparticles were washed in sterile milliQ water to remove the unbound antibody, collected, freeze dried and stored at 4 °C for future use.

2.2. Animals and experimental design

C57BL/6J mice were maintained in colony cages with free access to food and sterile water, under standardized housing conditions (natural light–dark cycle, temperature of 23 ± 1 °C, relative humidity of 55 ± 5%). All the animals used in the study were acclimatized to laboratory conditions prior to the experiments and were randomly assigned to the following experimental groups (n = 6).

1) Untreated control; 2) D-Gal disease group (120 mg/kg body weight (BW); 3) D-Gal + melatonin (1 mg/kg BW); 4) D-Gal + Void NPs (1.5 mg/kg BW); 5) D-Gal + SurR9-C84A NPs (1.5 mg/kg BW); and 6) D-Gal + TFN SurR9-C84A NPs (1.5 mg/kg BW). D-Gal was administered daily by intraperitoneal injection for 6 weeks and the treatments were given through intravenous route in the last two weeks. The dose of melatonin (1 mg/kg BW) was reported in the study of Shen et al. [28] while the rest were fixed based on a tolerated dose conducted. The entire *in vivo* study was performed strictly following the guidelines as recommended for the care and use of laboratory animals of the National Institutes of Health (NIH). The experimental protocol was approved by the Institutional animal ethical committee (IAEC), Kakatiya University, Warangal.

2.3. Behavioural tests

2.3.1. Locomotor activity

A majority of the CNS therapeutics influence the locomotor activity in both the animals and man and hence is a good indicative of the brain functioning. This activity is studied using an actophotometer embedded with the photoelectric cells that are connected in a circuit. The recordings were noted soon after the animal moves and cut offs the light beam falling on the photocell. On the test date, animals were placed individually in the activity cage and monitored before and after 30 min of drug administration for assessing the locomotor activity [29].

2.3.2. Rotarod test

The rotarod apparatus is a widely accepted experimental method for evaluating the locomotor coordination in mice as neurodegeneration is associated with a significant decline in motor control. In this study, a five-station accelerating rota-rod (model ENV-575M, St. Albans) has been adopted for testing the grip strength.

Initially, the animals were trained prior on the rota rod at a speed of 24 rpm for 2 min following which another trial is repeated. The mice were sufficiently trained before proceeding for actual recording post drug treatments. Each testing session consisted of at least 5 trials per mouse per day with a gap of 30 min between the trials. The recordings were made soon after the mice began to fall from the apparatus interrupting the infrared beam.

2.4. Gene analysis (see supplementary Section 1.3)

2.4.1. Immunohistochemistry for various markers (see supplementary Section 1.4)

2.4.1.1. Statistical analysis. One-way and two-way ANOVA with Tukey's post-hoc test was employed for calculating the statistical difference and the results with 'p' less than 0.05 were considered as statistically significant.

3. Results

3.1. Nanoparticle preparation and characterization

The prepared NPs were characterized for the shape and morphology using the scanning electron microscopy. As observed from Fig. 1A, all the prepared NPs were spherical in shape with an average size of 150 nm that are ideal for the brain penetration [24]. The NPs were then tested to see the integrity of the protein encapsulated, along with the successful binding of transferrin receptor antibody. The successful encapsulation of SurR9-C84A inside the NPs was clearly visible as observed from Fig. 1B. To differentiate this, the protein only (SurR9-C84A) and void nanoparticle gel images are also shown. Further, the NP surface modification was found to be around 74% (Fig. 1C) and this is also detectable with the presence of transferrin antibody heavy and light chains (Fig. 1B). The targeted NPs were also evaluated for internalization in the SK-N-SH neurons and were observed to be successfully uptaken within 30 min post-incubation (Fig. 1D).

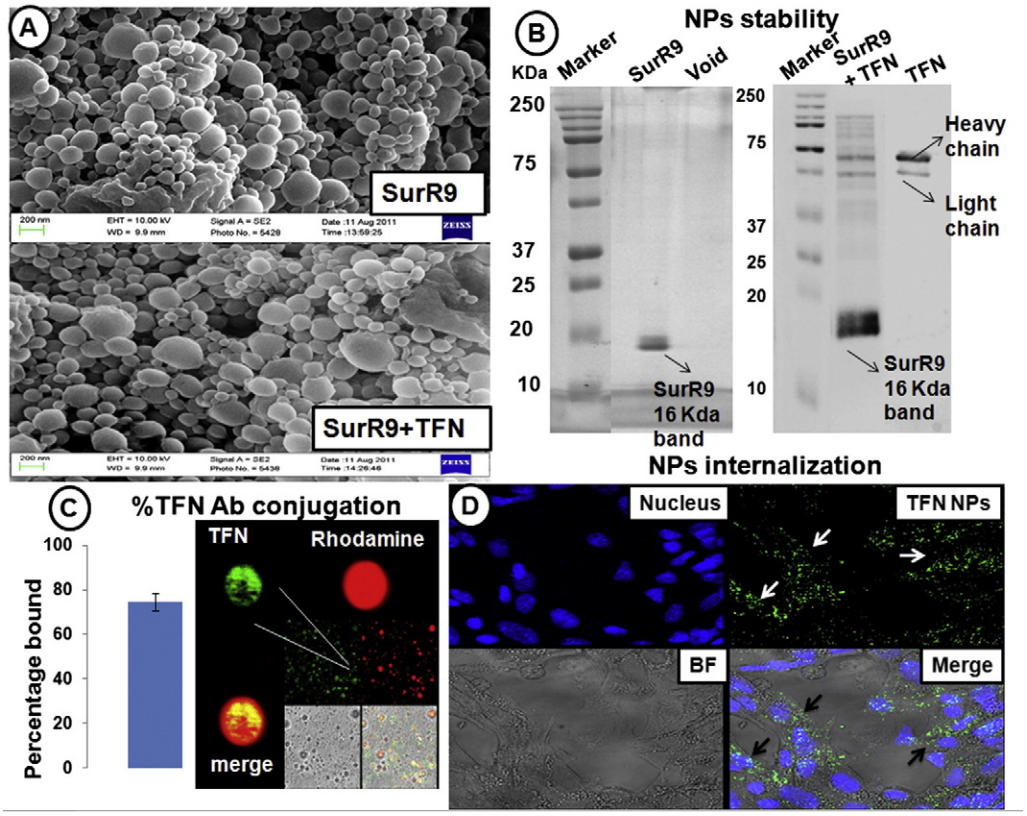

Fig. 1. Characterization of targeted nanoparticles. A) Scanning electron microscopic images of the prepared PLGA NPs. All of the images showed smooth spherical morphology with an average size of 150 nm. B) SDS-Gel image confirming the successful encapsulation of SurR9-C84A inside the nanoparticles. The targeted NPs were also observed to have the heavy and light chain bands of anti-transferrin receptor antibody confirming the successful surface modification. SurR9-C84A protein only and void nanoparticle bands are also shown. C) Confocal microscopic image of the anti-transferrin antibody conjugated SurR9-C84A loaded NPs. Rabbit anti-mouse FITC (green channel) showing the presence of antibody on the surface of the NPs. D) The targeted NPs were incubated with the differentiated SK-N-SH neurons and were found to be internalized within 30 min. Arrow heads indicating the internalized nanoparticles.

3.2. In vitro protective actions of SurR9-C84A against D-Galactose toxicity

Demonstrating its neuroprotective activity, SurR9-C84A was able rescue the neurons from the D-Gal induced toxicity. As observed from Fig. 2, D-Gal induced a significant 13.8 fold increment in the β-amyloid protein expression while pre-treatment with the SurR9-C84A prior to D-Gal insult lowered the expression by 4.5 folds ($p < 0.05$). The same was compared against the positive control, melatonin which showed a reduced expression of β-amyloid by 3.7 folds. In addition to this, D-Gal insults also showed a reduced expression of β-tubulin III (Fig. 2C), a neuronal integrity marker by 2.7 folds compared to the untreated control, while SurR9-C84A and melatonin increased its expression by 1.4 and 1.5 folds respectively post D-Gal insults (Fig. 2D).

3.3. Behavioural analysis and gene expression

The D-Gal induced effect on motor coordination was studied using the rotarod and the mice showed random grip strengths for the first four weeks where no treatments were started. However, during the treatment period (5th week), improvement in the grip strengths were observed for melatonin and SurR9 + TFN groups that showed a 1.24 and 1.28 folds improvement compared to the diseased control (Fig. 3A). The locomotory activity showed a drastic change in the 6th week, where D-Gal showed the least activity as counted by the photobeam interruptions. A noticeable improvement was however observed for melatonin, SurR9-C84A and SurR9 + TFN groups (Fig. 3B) with 1.3, 1.17, and 1.26 fold increased crossings. As observed from Fig. 3C, D-Gal induced the enhanced expression APP, APOE and GSK-3 by 16, 67 and 25 folds respectively indicating the degenerative onset. Also, the apoptotic marker caspase-3 showed a maxim of 46% increase in the disease control. However, SurR9-C84A treatment showed maximum expression of wild type survivin and its splice variant (Sur3β) along with the neuronal integrity markers NF 68 and NF 200. The targeted SurR9-C84A treatment was very effective in lowering the pathologic APP, GSK-3 and apoptotic caspase-3 markers (Fig. 3C).

3.4. Immunohistochemistry for various markers

As observed, the control group showed no abnormal neuronal cell morphology but the D-Gal insult group showed enlarged intercellular spaces, pyknotic nucleus, light cytoplasmic staining and capillaries surrounded by erythrocytes (Fig. 4A). However, an evident improvement in the neural cell morphology was observed in the treatment groups more specifically with the SurR9 + TFN group (Fig. 4A). The void only control, showed similar patterns as observed with D-Gal insult, confirming the effective protein therapy (Fig. 4A). Further substantiating the results, D-Gal only treated control showed intense immunoreactivity for pathologic β-amyloid, Cas-3 (Fig. 4A), excitatory amino acid transporter, glutamate and NMDA receptors (Fig. 4B) and endogenous survivin (Fig. 4C) while the neuronal integrity markers NF 68 and NF 200 showed a lighter reactivity (Fig. 4C). However, treatment groups significantly improved the neuronal recovery as observed from the stainings of survivin, NF 68 and NF 200 (Fig. 4C). Compared to the non-targeted treatment group, the targeted SurR9 + TFN was effective and showed a slightly improved outcome (Fig. 4A–D).

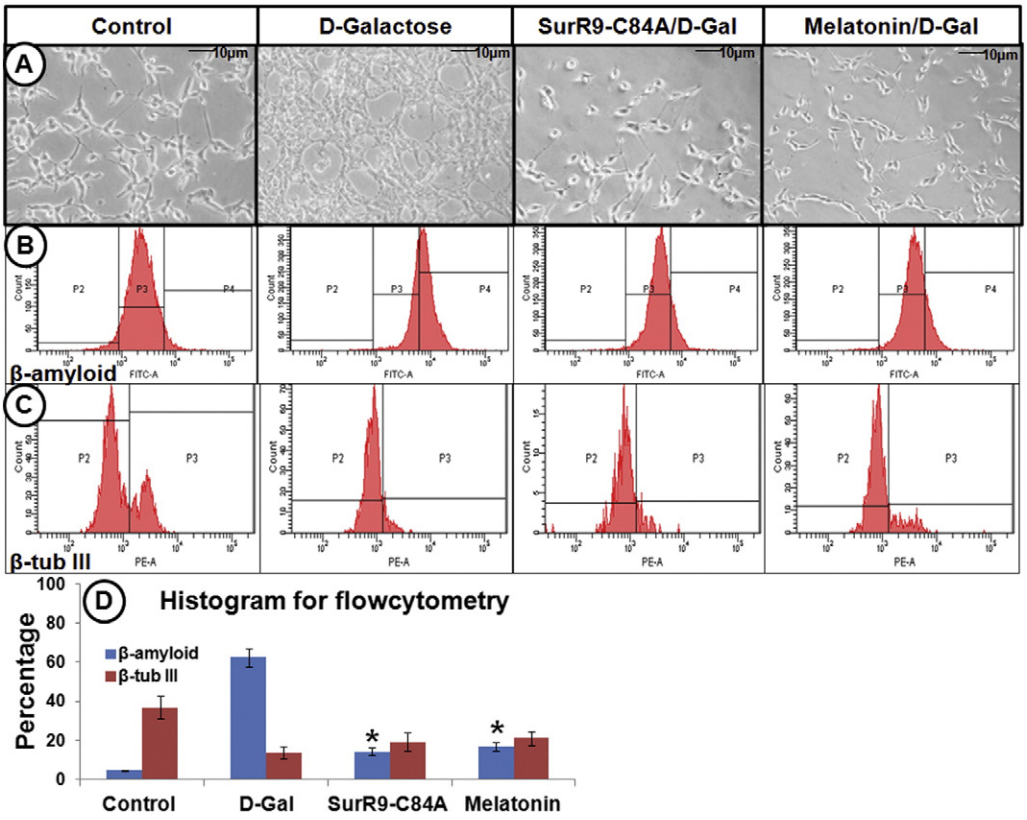

Fig. 2. Protective actions of SurR9-C84A against D-Galactose induced insults *in vitro*. A) Microscopic images of SK-N-SH neurons post D-Galactose insults; scale bar = 10 μm. B) Flowcytometry analysis for β-amyloid expression post D-Gal insults. C) Flowcytometry analysis for β-tubulin III expression post D-Gal insults. D) Histogram showing the flowcytometry for β-amyloid and β-tubulin III expression. Overall, D-Gal induced significant increase in the expression of β-amyloid and lowered the β-tubulin III expression that was respectively nullified by SurR9-C84A actions, *$p < 0.05$ is considered statistically significant.

3.5. Biodistribution of SurR9-C84A

As observed from Fig. 4E, a major proportion (~800 ng/ml) of the targeted anti-transferrin SurR9-C84A was accumulated in the brain. This is 25% more compared to the accumulation in any of the tissues considered and is because of the abundant availability of the TFN receptors in the brain [30]. Hence, it is believed that the surface functionalized SurR9-C84A have shown better permeation, bioavailability and efficacy compared to the non-conjugated SurR9-C84A treatment. Surprisingly, the non-conjugated SurR9-C84A showed very less brain permeation and is explained because of its enhanced accumulation in the bone, blood, liver and spleen (Fig. 4E).

3.6. Immunofluorescence for glial fibrillary acidic protein (GFAP)

To further substantiate the protective actions of the various proteins studied, immunofluorescence staining was performed for the GFAP protein. Surprisingly, GFAP was observed to be highly expressed in the D-Gal disease control that constituted to 4.8 folds increase compared to the untreated mice (Fig. 5A) $p < 0.001$.

Intriguing results were marked with the treated groups that showed a strong decrement in the GFAP levels denoting reduced occupancy of reactive astrocytes (Fig. 5A). Detailed expression is shown in Supplementary Figure S1A & B.

4. Discussion

The mutant SurR9-C84A protein belonging to the class of inhibitor of apoptotic proteins (IAPs) has shown to be potentially neuroprotective targeting the wild type survivin in the neurons. The mechanistic pathway behind its protection was reported as, neurons being postmitotic cells, possess negligible endogenous survivin pool and upon treatment, SurR9-C84A behaves indistinguishable to the wild type and shows its protective activity [27,31–33]. Hence, the nanoencapsulation of SurR9-C84A along with a batch of surface modified, anti-transferrin receptor antibody conjugated, SurR9-C84A NPs were formulated and their efficacy was evaluated for addressing the D-Gal insult. The prime reason for using the NPs is to provide stability to the protein therapeutics, while the conjugation with anti-transferrin receptor antibody guided the NPs for brain specific delivery. Transferrin is one of the abundantly available brain specific targets expressed on the brain capillary endothelium and hence is an attractive ligand for nanoparticle conjugation [30]. Considering the potential *in vitro* activity of SurR9-C84A, we tried to investigate its possible neuroprotective actions against D-Gal induced insults for which an extensive literature exists [34–37]. The basic mechanism behind the cause of neurodegeneration is explained as, chronic exposure of D-Gal leads to overproduction of ROS following its oxidative metabolism generating AGEs [38]. AGEs are considered as the resultant by-products of the addition reactions that occur between the reduced sugars (D-Gal in this case) and free amine groups present on the polypeptides and lipids. The dreadful events appear soon after the formation of AGEs and their binding to the receptors for AGEs (RAGE) in the cells and tissues.

Thus, it results in the protein aggregation that is highly implicated in AD [39]. On the other hand, to improve the drug availability inside the brain, surface modified, anti-transferrin receptor antibody conjugated SurR9-C84A NPs were used. Transferrin receptor is reported to be one of the specific receptor expressed on the brain endothelium and has attracted a lot of attention for fabricating brain targeted deliveries [40,41]. The characterization of NPs revealed that all of them have a size below 150 nm which is ideal for brain penetration (Fig. 1A) and

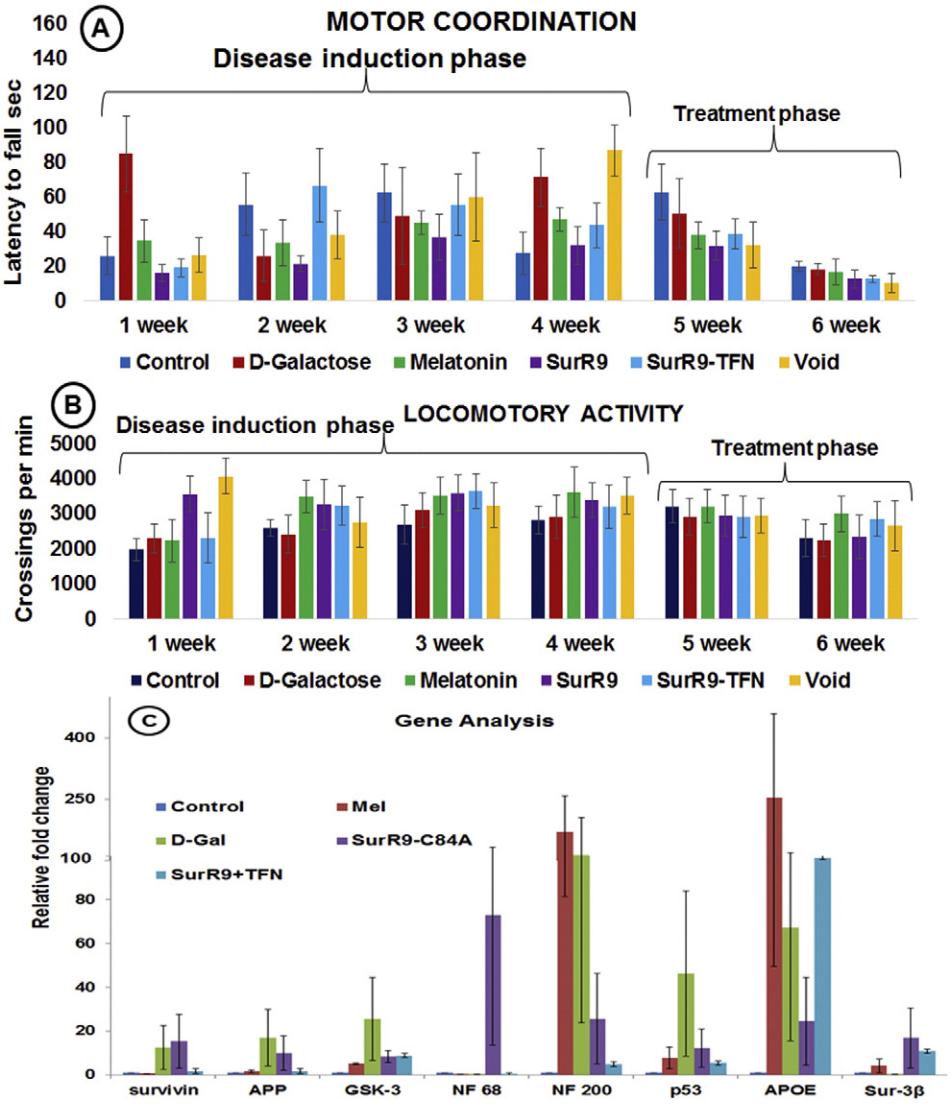

Fig. 3. The behavioural improvement following the treatment with various nanoformulations. A) The motor coordination following the insults with D-Gal and treatments were analysed for 6 weeks. For the first 4 weeks randomised grip strengths were observed but however, treatments with melatonin and SurR9 + TFN showed an improvement in the time spent by the mice. B) The locomotory activity also diminished following D-Gal insults but a noticeable recovery was observed for melatonin, SurR9-C84A and SurR9 + TFN groups. C) Gene expression analysis uncovered increased expression of genes involved in neuronal insult and protection. As observed from this figure (panel C), D-Gal induced the enhanced expression of pathologic (APP, APOE and GSK-3) and apoptotic genes (caspase-3) following D-Gal only insult. However, there was a drastic shift towards the enhanced expression of survival genes (wild type survivin, NF 68, NF 200) following SurR9-C84A treatments.

the proteins inside the NPs were stable (Fig. 1B). The surface modification achieved through the carbodiimide chemistry revealed successful TFN conjugation with almost 75% NPs showing the presence of TFN and showed an internalization of 90% upon incubation (Fig. 1D). Preliminarily, D-Gal induced insults were evaluated *in vitro*, where untreated D-Gal control showed enhanced, pathologic β-amyloid and reduced β-tubulin III expression. Contrast results were observed in the cells pre-treated with SurR9-C84A and positive control melatonin (Fig. 2A–D). However, only the TFN conjugated SurR9 NPs showed a significant improvement against the D-Gal induced oxidative stress (Supplementary Figure S2). The current results were also similar to previous reports where the D-Gal induced oxidative stress and β-amyloid expression were proportionate to each other (Fig. 4D) [42]. The exact mechanism of how D-Gal induces behavioural impairment is still unknown, but there are speculations that the oxidative stress induced neurodegeneration might be the reason behind it [4].

Interesting theory was also reported where a maximum behavioural impairment was observed at 120 mg/kg dose and self-limitation of this effect at >200 mg/kg [5]. When implied in this study, a progressive decline in the motor activity was observed reaching its peak in the 6th week. However, only the melatonin and SurR9 + TFN NPs treated groups were observed to be positively influenced in overcoming the behavioural compromise. D-Gal insults also reflected noticeable changes in the expression of APP, GSK-3 and Cas-3, APP and GSK-3. All of these are the pathologic hallmarks of AD associated with the β-amyloid aggregation and tau phosphorylation [43]. Surprisingly, D-Gal also showed an elevated expression of survivin and mature differential marker that has been predicted as the neuronal survival responses. With respect to the treatments, all of them were very effective in lowering the pathologic markers and in particular SurR9-C84A showed an enhanced expression of survivin, integrity marker NF 68 and its splice variant Sur3β indicating extensive protective activity (Fig. 4C). The morphology analysis depicted a clear picture of neuronal degeneration evident with pyknotic nuclei, reduced cytoplasmic staining, enlarged vacuoles and erythrocytes post D-Gal insults (Fig. 4A). Further, histology results revealed enhanced β-amyloid, cas-3, survivin and reduced NF 68 and NF 200 expression substantiating D-Gal induced neuronal injury. Interestingly, the EAAT2 expression was also observed to be lowered

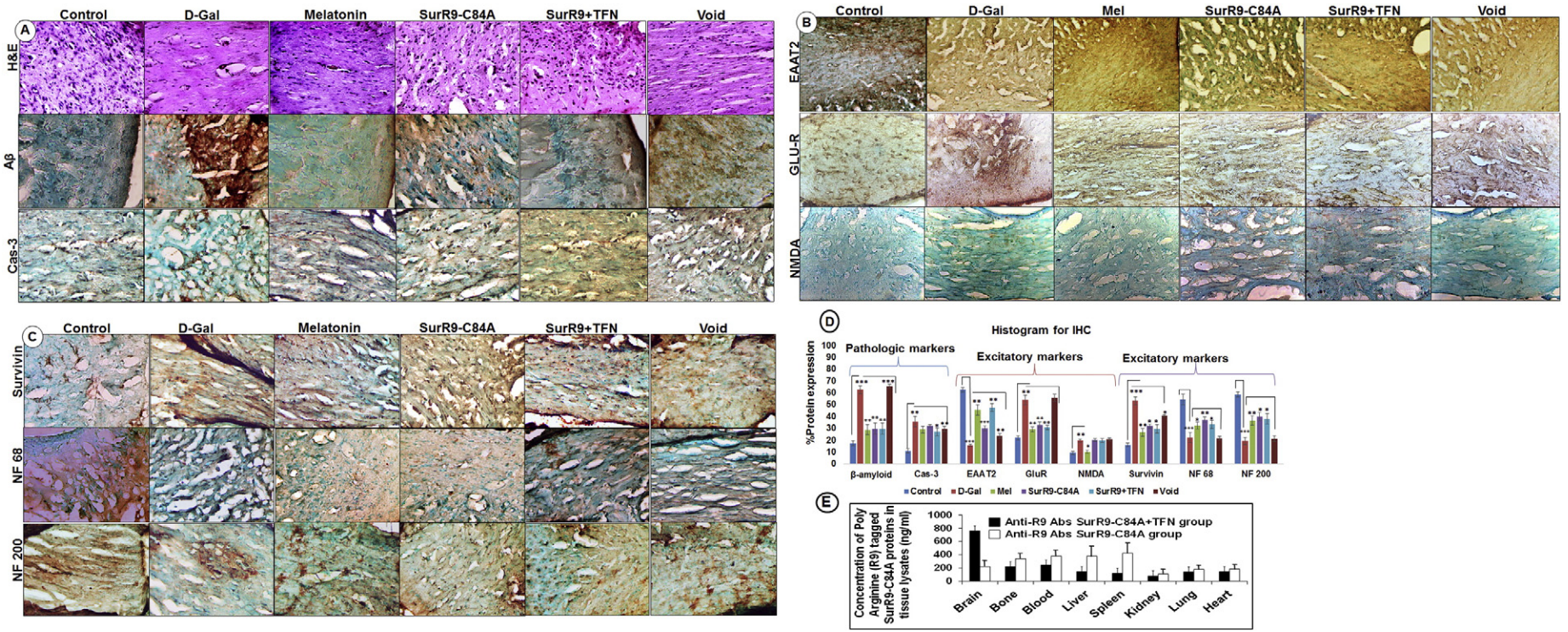

Fig. 4. Neuroprotective activity of the nanoformulations. A) D-Gal induced insults showed pyknotic nuclei, lighter cytoplasmic staining (H & E) and increased expression of pathologic β-amyloid and Cas-3 expression. Arrow head showing the capillaries surrounded by erythrocytes B) Treatments showed reduced expression of excitatory amino acid transporter, glutamate and NMDA receptors in contrast to D-Gal insults. C) Neuronal recovery following the enhanced expression of integrity markers survivin, neurofilament 68 and 200 post treatments. The representative images from coronal brain sections are presented; $n = 3$; scale bar = 50 μm. All the images were shown in 40× objective. D) Histogram showing the comparative expression of pathologic and integrity markers. E) Biodistribution of anti-transferrin antibody conjugated and non-conjugated SurR9-C84A nanoparticles. SurR9-C84A with TFN antibody showed a brain specific localization and therefore has shown a maximum therapeutic outcome. $^{*}p < 0.05$, $^{**}p < 0.01$, and $^{***}p < 0.001$ are considered statistically significant.

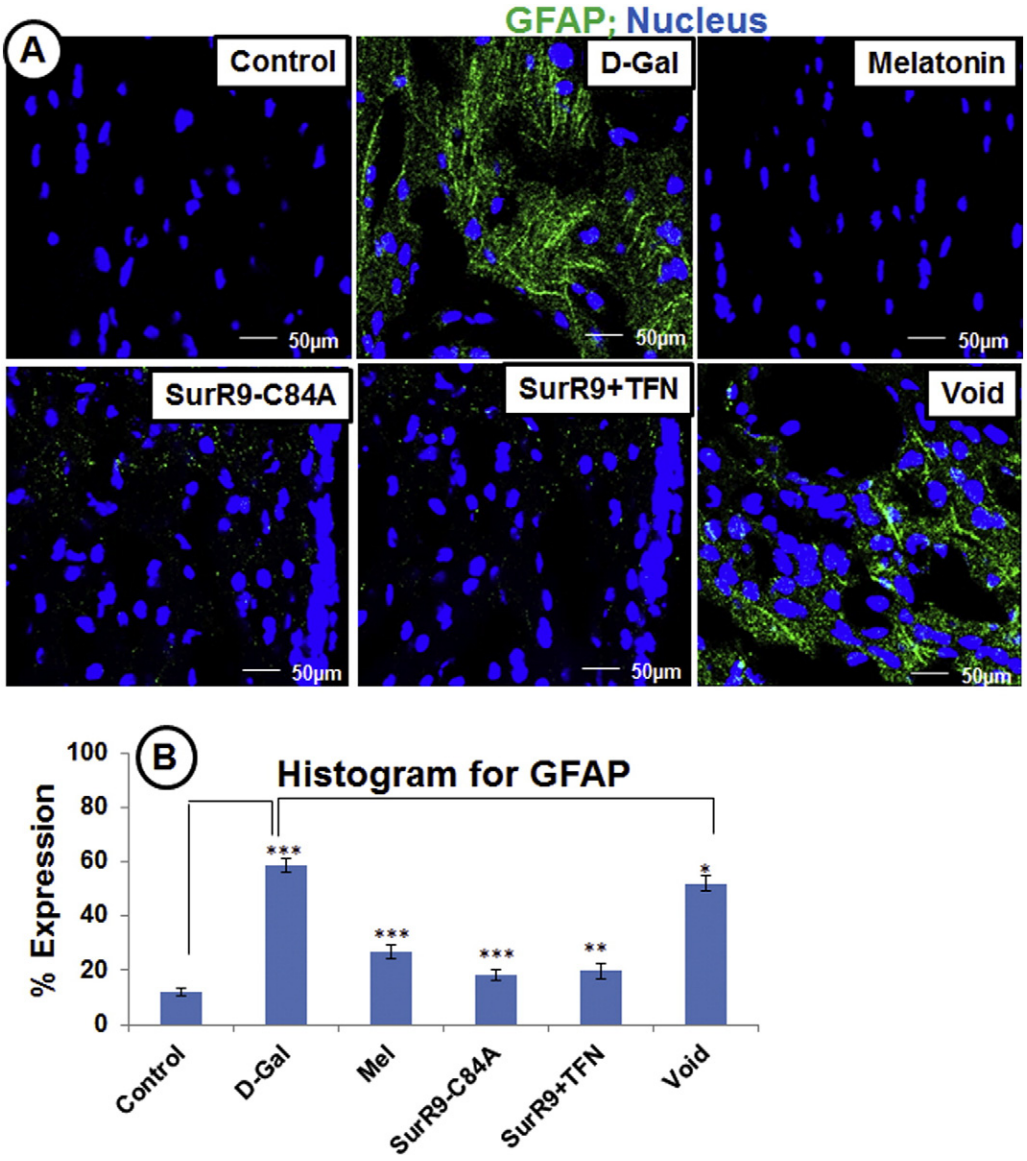

Fig. 5. Reduced reactive astrogliosis. A) Immunofluorescence confirmed the astrocytes reactivity following D-Gal insults with enhanced GFAP expression. The treatments however were effective in reducing the GFAP expression and were evident with the reduced FITC intensity (green channel). The representative images from coronal brain sections are presented; scale bar = 0–50 µm. All the images were shown in 40× objective. B) Histogram for GFAP expression. See supplementary Figs. S1A & S1B for detailed information.

in the disease control compared to the treatments, linking the disease severity to the glutamate clearance. EAAT2 is a vital glutamate transporter regulating its clearance, Ca^{2+} overload and several neurodegenerative studies have documented reduced EAAT2 expression [44,45].

Glutamate receptors showed an enhanced expression following D-Gal insults but the other excitatory receptor, NMDA was not significantly affected proving the excess glutamate involvement in this study (Fig. 4B). However, treatments showed contradicting D-Gal insults and showed much improved neuronal health (Fig. 4A-D).

The biodistribution studies also confirmed the enhanced brain specific permeation of anti-transferrin antibody conjugated SurR9-C84A and it is believed to be the reason behind improved therapeutic outcome (Fig. 4E). GFAP, a reactive astrocyte marker has also showed a differential expression with and without treatments post D-Gal insults. Astrocytes represent the primary glial cell population and play a key role in maintaining the neuronal homeostasis. However, in the instances of neurodegenerative insults they respond viciously initiating the inflammatory reactions, neurotoxic secretions and express elevated levels of GFAP marking the astrogliosis phenomenon [46]. Altogether, the *in vitro* results were optimistic and hence the protective effects of the nanoformulations were evaluated *in vivo*. In the present study, we used melatonin as a positive control to compare the efficacy of treatment groups, as it had strong anti-oxidant activity protecting the neurons [47] (Supplementary Figure S2). To conclude, SurR9-C84A NPs showed promising activity modifying the oxidative stress and abrogated the neuronal degeneration providing a basis for future therapeutic approach (Fig. 6).

5. Conclusion

The current study shows that chronic D-Gal administration induces oxidative stress and neurodegeneration associated with behavioural compromise. As a proof of concept, we have shown for the very first time that the surface functionalization of biodegradable, PLGA nanocarriers decorated with the anti-transferrin receptor antibodies is a promising approach for enabling the permeation and delivery of

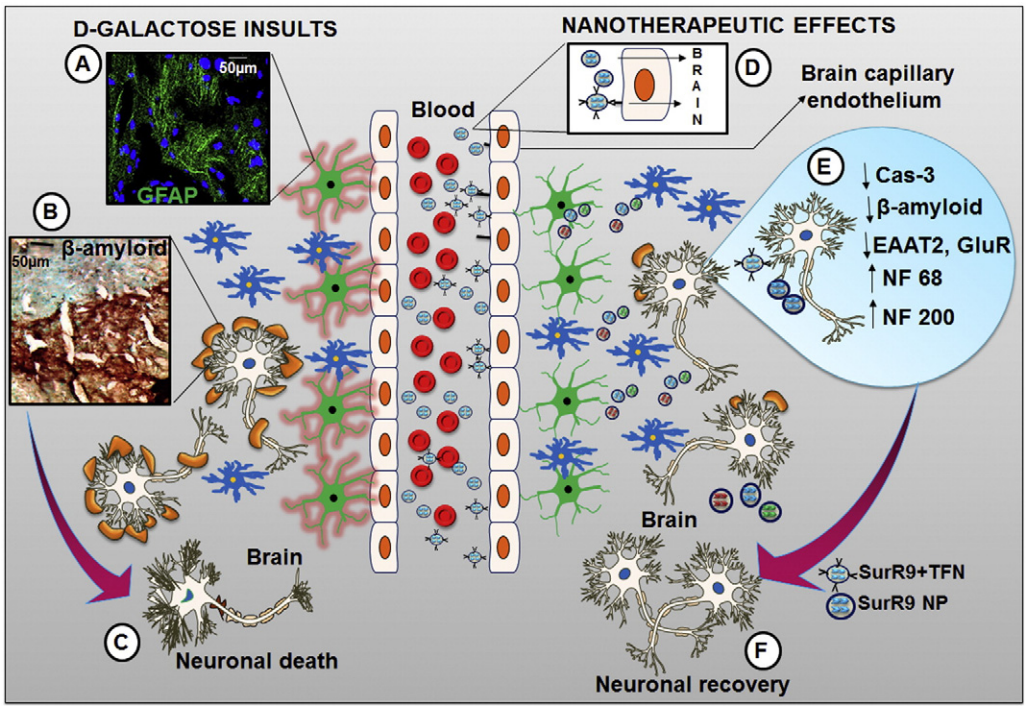

Fig. 6. Schematic representation of neuroprotective effect of nanoformulations. A) Reactive astrocytes with GFAP expression. B) Oxidative stress induced β-amyloid expression. C) Neuronal damage. D) Small sized SurR9-C84A nanoparticles permeate through the brain capillary endothelium while the anti-transferrin receptor antibody conjugated SurR9-C84A nanoparticles internalized *via* the receptor mediated endocytosis. E) Neuroprotective effect. F) Neuronal recovery.

SurR9-C84A inside the brain through BBB. Moreover, the NPs also enhanced the bioavailability of SurR9-C84A, thus enabling the differentiation and viability of the neurons. Altogether, the current report on the neuroprotective activity of SurR9-C84A-NPs is the first of its kind and future studies warrant the study of transferrin targeted nano-aptamers for further evaluation.

Author's contributions

BS was involved in study design, performed gene analysis, histology, imaging, analysed data, and drafted the manuscript. PN participated in disease induction and behavioural studies. RKK participated in study design and data analysis. JRK participated in study design, coordinated and designed the research. All authors read and accepted the final manuscript.

Transparency document

The Transparency document associated with this article can be found, in the online version.

Conflict of interest

The authors have no potential conflict of interest.

Acknowledgements

The authors would like to thank the Australia–India Strategic Research Fund (AISRF, BF030016/42), Deakin University Postgraduate Research Scholarship and the National Health and Medical Research Council (NHMRC, APP1050286) for financial support. No writing assistance was utilized in the production of this manuscript.

Appendix A. Supplementary data

Supplementary data to this article can be found online at http://dx.doi.org/10.1016/j.bbadis.2015.08.015.

References

[1] X. Cui, L. Wang, P. Zuo, Z. Han, Z. Fang, W. Li, J. Liu, D-galactose-caused life shortening in *Drosophila melanogaster* and *Musca domestica* is associated with oxidative stress, Biogerontology 5 (2004) 317–325.
[2] R.G. Jordens, M.D. Berry, C. Gillott, A.A. Boulton, Prolongation of life in an experimental model of aging in *Drosophila melanogaster*, Neurochem. Res. 24 (1999) 227–233.
[3] H.B. Deng, D.P. Cui, J.M. Jiang, Y.C. Feng, N.S. Cai, D.D. Li, Inhibiting effects of *Achyranthes bidentata* polysaccharide and *Lycium barbarum* polysaccharide on nonenzyme glycation in D-galactose induced mouse aging model, Biomed. Environ. Sci. 16 (2003) 267–275.
[4] H. Wei, L. Li, Q. Song, H. Ai, J. Chu, W. Li, Behavioural study of the D-galactose induced aging model in C57BL/6J mice, Behav. Brain Res. 157 (2005) 245–251.
[5] S.C. Ho, J.H. Liu, R.Y. Wu, Establishment of the mimetic aging effect in mice caused by D-galactose, Biogerontology 4 (2003) 15–18.
[6] H. Lei, B. Wang, W.P. Li, Y. Yang, A.W. Zhou, M.Z. Chen, Anti-aging effect of astragalosides and its mechanism of action, Acta Pharmacol. Sin. 24 (2003) 230–234.
[7] X. Song, M. Bao, D. Li, Y.M. Li, Advanced glycation in D-galactose induced mouse aging model, Mech. Ageing Dev. 108 (1999) 239–251.
[8] J. Tian, K. Ishibashi, K. Reiser, R. Grebe, S. Biswal, P. Gehlbach, J.T. Handa, Advanced glycation endproduct-induced aging of the retinal pigment epithelium and choroid: a comprehensive transcriptional response, Proc. Natl. Acad. Sci. U. S. A. 102 (2005) 11846–11851.
[9] X. Cui, P. Zuo, Q. Zhang, X. Li, Y. Hu, J. Long, L. Packer, J. Liu, Chronic systemic D-galactose exposure induces memory loss, neurodegeneration, and oxidative damage in mice: protective effects of R-alpha-lipoic acid, J. Neurosci. Res. 84 (2006) 647–654.
[10] A. Kumar, A. Prakash, S. Dogra, Naringin alleviates cognitive impairment, mitochondrial dysfunction and oxidative stress induced by D-galactose in mice, Food Chem. Toxicol. 48 (2010) 626–632.
[11] J.F. Turrens, Mitochondrial formation of reactive oxygen species, J. Physiol. 552 (2003) 335–344.
[12] K. Troulinaki, N. Tavernarakis, Neurodegenerative conditions associated with ageing: a molecular interplay? Mech. Ageing Dev. 126 (2005) 23–33.
[13] J.W. Baynes, The role of AGEs in aging: causation or correlation, Exp. Gerontol. 36 (2001) 1527–1537.
[14] P. Candela, F. Gosselet, J. Saint-Pol, E. Sevin, M.C. Boucau, E. Boulanger, R. Cecchelli, L. Fenart, Apical-to-basolateral transport of amyloid-beta peptides through blood-brain barrier cells is mediated by the receptor for advanced glycation end-products and is restricted by P-glycoprotein, J. Alzheimers Dis. 22 (2010) 849–859.

[15] C. Sims-Robinson, B. Kim, A. Rosko, E.L. Feldman, How does diabetes accelerate Alzheimer disease pathology? Nat. Rev. Neurol. 6 (2010) 551–559.
[16] A. Liu, Y. Ma, Z. Zhu, Protective effect of selenoarginine against oxidative stress in D-galactose-induced aging mice, Biosci. Biotechnol. Biochem. 73 (2009) 1461–1464.
[17] Z.F. Wang, J. Wang, H.Y. Zhang, X.C. Tang, Huperzine A exhibits anti-inflammatory and neuroprotective effects in a rat model of transient focal cerebral ischemia, J. Neurochem. 106 (2008) 1594–1603.
[18] S.Z. Zhong, Q.H. Ge, R. Qu, Q. Li, S.P. Ma, Paeonol attenuates neurotoxicity and ameliorates cognitive impairment induced by d-galactose in ICR mice, J. Neurol. Sci. 277 (2009) 58–64.
[19] J.L. Cummings, Alzheimer's disease, N. Engl. J. Med. 351 (2004) 56–67.
[20] J.R. Kanwar, B. Sriramoju, R.K. Kanwar, Neurological disorders and therapeutics targeted to surmount the blood-brain barrier, Int. J. Nanomedicine 7 (2012) 3259–3278.
[21] J.R. Kanwar, X. Sun, V. Punj, B. Sriramoju, R.R. Mohan, S.F. Zhou, A. Chauhan, R.K. Kanwar, Nanoparticles in the treatment and diagnosis of neurological disorders: untamed dragon with fire power to heal, Nanomedicine 8 (2012) 399–414.
[22] K. Hu, Y. Shi, W. Jiang, J. Han, S. Huang, X. Jiang, Lactoferrin conjugated PEG-PLGA nanoparticles for brain delivery: preparation, characterization and efficacy in Parkinson's disease, Int. J. Pharm. 415 (2011) 273–283.
[23] J. Li, C. Zhang, J. Li, L. Fan, X. Jiang, J. Chen, Z. Pang, Q. Zhang, Brain delivery of NAP with PEG-PLGA nanoparticles modified with phage display peptides, Pharm. Res. 30 (2013) 1813–1823.
[24] B. Sriramoju, R.K. Kanwar, J.R. Kanwar, Nanoformulated cell-penetrating survivin mutant and its dual actions, Int. J. Nanomedicine 9 (2014) 3279–3298.
[25] X. Zhang, G. Chen, L. Wen, F. Yang, A.L. Shao, X. Li, W. Long, L. Mu, Novel multiple agents loaded PLGA nanoparticles for brain delivery via inner ear administration: in vitro and in vivo evaluation, Eur. J. Pharm. Sci. 48 (2013) 595–603.
[26] M. Karasek, Melatonin, human aging, and age-related diseases, Exp. Gerontol. 39 (2004) 1723–1729.
[27] K.R, B. Sriramoju, J.R. Kanwar, Nanoformulated cell-penetrating survivin mutant and its dual actions, Int. J. Nanomedicine 9 (2014) 3279–3298.
[28] Y.X. Shen, S.Y. Xu, W. Wei, X.X. Sun, J. Yang, L.H. Liu, C. Dong, Melatonin reduces memory changes and neural oxidative damage in mice treated with D-galactose, J. Pineal Res. 32 (2002) 173–178.
[29] H.G. S.B. Vogel, J. Sandow, et al., Drug Effects on Learning and Memory, Springer, Berlin, 2002.
[30] K. Holloway, H. Sade, I.A. Romero, D. Male, Action of transcription factors in the control of transferrin receptor expression in human brain endothelium, J. Mol. Biol. 365 (2007) 1271–1284.
[31] S. Baratchi, R.K. Kanwar, C.H. Cheung, J.R. Kanwar, Proliferative and protective effects of SurR9-C84A on differentiated neural cells, J. Neuroimmunol. 227 (2010) 120–132.
[32] S. Baratchi, R.K. Kanwar, J.R. Kanwar, Survivin mutant protects differentiated dopaminergic SK-N-SH cells against oxidative stress, PLoS One 6 (2011), e15865.
[33] S. Baratchi, R.K. Kanwar, J.R. Kanwar, Novel survivin mutant protects differentiated SK-N-SH human neuroblastoma cells from activated T-cell neurotoxicity, J. Neuroimmunol. 233 (2011) 18–28.
[34] X. Cui, P. Zuo, Q. Zhang, X. Li, Y. Hu, J. Long, L. Packer, J. Liu, Chronic systemic D-galactose exposure induces memory loss, neurodegeneration, and oxidative damage in mice: protective effects of R-alpha-lipoic acid, J. Neurosci. Res. 83 (2006) 1584–1590.
[35] L. Hao, H. Huang, J. Gao, C. Marshall, Y. Chen, M. Xiao, The influence of gender, age and treatment time on brain oxidative stress and memory impairment induced by D-galactose in mice, Neurosci. Lett. 571C (2014) 45–49.
[36] X. Hua, M. Lei, J. Ding, Q. Han, G. Hu, M. Xiao, Pathological and biochemical alterations of astrocytes in ovariectomized rats injected with D-galactose: a potential contribution to Alzheimer's disease processes, Exp. Neurol. 210 (2008) 709–718.
[37] M. Lei, Y. Su, X. Hua, J. Ding, Q. Han, G. Hu, M. Xiao, Chronic systemic injection of D-galactose impairs the septohippocampal cholinergic system in rats, Neuroreport 19 (2008) 1611–1615.
[38] A. Kumar, A. Prakash, S. Dogra, *Centella asiatica* attenuates D-Galactose-induced cognitive impairment, oxidative and mitochondrial dysfunction in mice, Int. J. Alzheimers Dis. 2011 (2011) 347569.
[39] L.F. Lue, D.G. Walker, L. Brachova, T.G. Beach, J. Rogers, A.M. Schmidt, D.M. Stern, S.D. Yan, Involvement of microglial receptor for advanced glycation endproducts (RAGE) in Alzheimer's disease: identification of a cellular activation mechanism, Exp. Neurol. 171 (2001) 29–45.
[40] Y. Cui, Q. Xu, P.K. Chow, D. Wang, C.H. Wang, Transferrin-conjugated magnetic silica PLGA nanoparticles loaded with doxorubicin and paclitaxel for brain glioma treatment, Biomaterials 34 (2013) 8511–8520.
[41] W. Guo, A. Li, Z. Jia, Y. Yuan, H. Dai, H. Li, Transferrin modified PEG-PLA-resveratrol conjugates: in vitro and in vivo studies for glioma, Eur. J. Pharmacol. 718 (2013) 41–47.
[42] A.C. Fonseca, E. Ferreiro, C.R. Oliveira, S.M. Cardoso, C.F. Pereira, Activation of the endoplasmic reticulum stress response by the amyloid-beta 1–40 peptide in brain endothelial cells, Biochim. Biophys. Acta 1832 (2013) 2191–2203.
[43] Y.H. Suh, F. Checler, Amyloid precursor protein, presenilins, and alpha-synuclein: molecular pathogenesis and pharmacological applications in Alzheimer's disease, Pharmacol. Rev. 54 (2002) 469–525.
[44] C.K. Colton, Q. Kong, L. Lai, M.X. Zhu, K.I. Seyb, G.D. Cuny, J. Xian, M.A. Glicksman, C.L. Lin, Identification of translational activators of glial glutamate transporter EAAT2 through cell-based high-throughput screening: an approach to prevent excitotoxicity, J. Biomol. Screen. 15 (2010) 653–662.
[45] C.L. Lin, Q. Kong, G.D. Cuny, M.A. Glicksman, Glutamate transporter EAAT2: a new target for the treatment of neurodegenerative diseases, Future Med. Chem. 4 (2012) 1689–1700.
[46] L.F. Eng, R.S. Ghirnikar, GFAP and astrogliosis, Brain Pathol. 4 (1994) 229–237.
[47] H.M. Hsieh, W.M. Wu, M.L. Hu, Soy isoflavones attenuate oxidative stress and improve parameters related to aging and Alzheimer's disease in C57BL/6J mice treated with D-galactose, Food Chem. Toxicol. 47 (2009) 625–632.